AMERICAN SOCIETY FOR MICROBIOLOGY | Infection and Immunity

Porphyromonas gulae Has Virulence and Immunological Characteristics Similar to Those of the Human Periodontal Pathogen *Porphyromonas gingivalis*

Jason C. Lenzo, Neil M. O'Brien-Simpson, Rebecca K. Orth, Helen L. Mitchell, Stuart G. Dashper, Eric C. Reynolds

Oral Health Cooperative Research Centre, Melbourne Dental School, Bio21 Institute, The University of Melbourne, Melbourne, Victoria, Australia

Periodontitis is a significant problem in companion animals, and yet little is known about the disease-associated microbiota. A major virulence factor for the human periodontal pathogen *Porphyromonas gingivalis* is the lysyl- and arginyl-specific proteolytic activity of the gingipains. We screened several *Porphyromonas* species isolated from companion animals—*P. asaccharolytica*, *P. circumdentaria*, *P. endodontalis*, *P. levii*, *P. gulae*, *P. macacae*, *P. catoniae*, and *P. salivosa*—for Lys- and Arg-specific proteolytic activity and compared the epithelial and macrophage responses and induction of alveolar bone resorption of the protease active species to that of *Porphyromonas gingivalis*. Only *P. gulae* exhibited Lys-and Arg-specific proteolytic activity. The genes encoding the gingipains (RgpA/B and Kgp) were identified in the *P. gulae* strain ATCC 51700 and all publicly available 12 draft genomes of *P. gulae* strains. *P. gulae* ATCC 51700 induced levels of alveolar bone resorption in an animal model of periodontitis similar to those in *P. gingivalis* W50 and exhibited a higher capacity for autoaggregation and binding to oral epithelial cells with induction of apoptosis. Macrophages (RAW 264.7) were found to phagocytose *P. gulae* ATCC 51700 and the fimbriated *P. gingivalis* ATCC 33277 at similar levels. In response to *P. gulae* ATCC 51700, macrophages secreted higher levels of cytokines than those induced by *P. gingivalis* ATCC 33277 but lower than those induced by *P. gingivalis* W50, except for the interleukin-6 response. Our results indicate that *P. gulae* exhibits virulence characteristics similar to those of the human periodontal pathogen *P. gingivalis* and therefore may play a key role in the development of periodontitis in companion animals.

Periodontitis is well known to occur in companion animals, particularly in dogs (1). The prevalence and severity of the disease increase with age (1). Chronic periodontitis, as diagnosed by increased periodontal pocket depth and/or gingival recession (1), has been shown to be present in 82% of dogs aged 6 to 8 years and in 96% of dogs aged 12 to 14 years (2). Black-pigmented anaerobic bacteria are commonly isolated from the periodontal pockets of dogs (3–5), with many of the isolates being identified as *Porphyromonas* species: *P. asaccharolytica*, *P. circumdentaria*, *P. endodontalis*, *P. levii*, *P. gulae*, *P. macacae*, *P. catoniae*, and *P. salivosa*. Of these species, *Porphyromonas gulae* has been found to be the predominant species (6). In humans, chronic periodontitis is an inflammatory disease of the supporting tissues of the teeth, which results in the destruction of the alveolar bone and the supporting tissue (7). It has been estimated to affect up to 25% of the dentate population, with severe forms affecting 5 to 6% and prevalence increasing with age (8, 9). Although the etiology of chronic periodontitis is multifactorial, evidence suggests that the levels of specific Gram-negative, anaerobic, black-pigmented bacteria in the subgingival plaque biofilm play a major role in the pathogenesis of human disease (10). Of these bacteria, *Porphyromonas gingivalis* has been implicated as a major etiological agent (11) now described as a "keystone pathogen" (12).

To date, the majority of work on *P. gulae* has focused on describing the bacterium as part of the dog oral microbiome associated with periodontitis rather than investigating its virulence characteristics. *P. gulae* is an obligate anaerobe that is a non-spore-forming, nonmotile, Gram-negative coccobacillus (13). It has been isolated from various mammals, including the common human companions cats and dogs (13). *P. gulae* is rarely isolated from healthy animals but is commonly isolated from animals with active periodontitis (14, 15) and is rarely found in humans (16). *P. gulae* has been reported to have fimbrial proteins (FimA) that are similar to the FimA proteins of *P. gingivalis* (17). Two forms of FimA (types A and B) that may confer virulence have been identified, with type B inducing greater systemic inflammation in a mouse abscess model (18). Mouse models have been used to examine the pathology of *P. gulae* oral infection and to determine the efficacy of inactivated whole-cell vaccines (19). Mice orally inoculated with *P. gulae* generate a bacterium-specific IgG response and develop alveolar bone resorption similar to that reported for *P. gingivalis* (20, 21). Subcutaneous injection of an inactivated whole-cell *P. gulae* vaccine was found to ameliorate alveolar bone resorption (19, 22), and this work formed the basis of a companion animal vaccine for periodontitis. However, this whole-cell vaccine, marketed by Pfizer, has been discontinued (23).

Received 10 December 2015 **Returned for modification** 15 February 2016
Accepted 15 June 2016

Accepted manuscript posted online 27 June 2016

Citation Lenzo JC, O'Brien-Simpson NM, Orth RK, Mitchell HL, Dashper SG, Reynolds EC. 2016. *Porphyromonas gulae* has virulence and immunological characteristics similar to those of the human periodontal pathogen *Porphyromonas gingivalis*. Infect Immun 84:2575–2585. doi:10.1128/IAI.01500-15.

Editor: B. A. McCormick, The University of Massachusetts Medical School

Address correspondence to Eric C. Reynolds, e.reynolds@unimelb.edu.au.

J.C.L. and N.M.O.-S. contributed equally to this article.

Supplemental material for this article may be found at http://dx.doi.org/10.1128/IAI.01500-15.

Given the high incidence of periodontal disease in companion animals and the emerging data that link *P. gulae* to disease, very little research has been conducted on this bacterium and its virulence characteristics. In order to understand the disease process in animals, key virulence factors should be identified and the interaction of the bacterium with the host characterized. In this study, we examined companion animal periodontitis-associated bacteria for proteolytic activity, a known virulence factor for the human periodontal pathogen *P. gingivalis* (24), and characterized the interaction of *P. gulae* with oral epithelial cells and innate immune cells.

MATERIALS AND METHODS

Bacterial strains and growth conditions. *Porphyromonas gulae* (ATCC 51700) and *P. endodontalis* (ATCC 35406) were grown in batch culture in Todd-Hewitt broth (36.4 g/liter; Oxoid, Hampshire, England) supplemented with cysteine (1 g/liter; Sigma-Aldrich, New South Wales, Australia), hemin (5 mg/liter; Sigma-Aldrich), and menadione (1 mg/liter; Sigma-Aldrich). *P. asaccharolytica* (ATCC 27067), *P. catoniae* (ATCC 51270), *P. circumdentaria* (ATCC 51356), *P. levii* (ATCC 29147), *P. macacae* (ATCC 33141), and *P. salivosa* (ATCC 49407) were grown in batch culture in brain heart infusion medium (37.0 g/liter; Oxoid) supplemented with cysteine (1 g/liter; Sigma-Aldrich), hemin (5 mg/liter; Sigma-Aldrich), and menadione (1 mg/liter; Sigma-Aldrich). *Porphyromonas gingivalis* W50 and ATCC 33277 were grown and harvested as previously described (25). Cultures were grown in an MK3 anaerobic workstation (Don Whitley Scientific, New South Wales, Australia) at 37°C with a gas composition of 5% H_2 and 10% CO_2 in N_2 for 24 to 48 h. All bacteria were harvested during the late exponential phase, as determined by growth curve, and the optical density was measured at 650 nm using a spectrophotometer (Varian model Cary 50; Bio UV/Spectrophotometer, California). Bacterial concentrations were determined using a live/dead fluorescence system. The green fluorescent DNA dye Syto9 (Life Sciences Pty, Ltd., New South Wales, Australia) was used in conjunction with propidium iodide (PI; Life Sciences) to determine viable bacteria, which were counted on a Cell Lab Quanta SC flow cytometer (Beckman Coulter, Inc., New South Wales, Australia). The Quanta SC is equipped with an argon ion laser operating at an excitation wavelength of 488 nm with green fluorescence measured through a 525-nm filter (FL1) and red fluorescence measured through a 575-nm filter (FL2). When passaged on solid media, all species were grown on horse blood agar (40 g/liter blood agar base no. 2, 10% [vol/vol] defribrinated horse blood, and 1 mg/liter menadione) for 4 to 8 days.

Arg-specific and Lys-specific proteolytic activity assays. Arg-specific and Lys-specific protease assays were carried out as previously described (26). Briefly, benzoyl-L-Arg-*p*-nitroanilide (BA*p*NA; Sigma) and benzyloxycarbonyl-L-Lys-*p*-nitroanilide (Lys*p*NA; Novabiochem) were used to assay the Arg- and Lys-specific proteolytic activity of *P. asaccharolytica*, *P. catoniae*, *P. circumdentaria*, *P. endodontalis*, *P. levii*, *P. gulae*, *P. macacae*, *P. salivosa*, and *P. gingivalis* (W50 and ATCC 33277). Whole bacterial cells (10^8 bacteria/ml) were incubated with 100 mM L-cysteine in TC150 buffer (150 mM NaCl, 50 mM Tris-HCl, 5 mM $CaCl_2$ [pH 7.4]) for 10 min at 37°C before the addition of BA*p*NA or Lys*p*NA (Sigma-Aldrich). The optical density at 405 nm (OD_{405}) was measured on a Wallac Victor3 plate spectrophotometer (PerkinElmer Pty, Ltd., New South Wales, Australia) every 4 s for 120 s. The protease activity was expressed as U/ml, which represents the μmol of BA*p*NA or Lys*p*NA hydrolyzed per min per ml. A Student *t* test was used to determine statistical differences, and a *P* value of <0.05 was considered significant.

DNA sequencing. The predicted *kgp* gene from the Loup 1 *P. gulae* type strain (ATCC 51700) (13) was validated using Sanger sequencing. Primers were designed using Primer3 v2.3.4 (27). Primer sets were designed to amplify 500-bp regions, and repeat-region coordinates were used to exclude target sites (see Table S1 in the supplemental material). The primers kgp_F1 and kgp_Rii were used to produce a 5.2-kb amplicon for each strain, which was quantified and used as the template with each of the primers listed for capillary electrophoresis sequencing at The Melbourne Translational Genomics Platform.

Autoaggregation assay. The ability of bacteria to autoaggregate was measured using an assay adapted from Nishiyama et al. (28). Briefly, bacteria were grown and harvested as described above before being washed twice with 20 mM phosphate-buffered saline (PBS; pH 6.0) and resuspended in 20 mM PBS. The OD_{650} of the cell suspension was measured and adjusted to an OD_{650} of 1.0. Aliquots (2 ml) were then added to optically clear polystyrene tubes (BD Falcon, New South Wales, Australia), gently mixed, and then incubated at 37°C. The OD_{650} was measured every 10 min, with autoaggregation being observed as a decrease in the optical density.

Labeling of bacteria. *P. gulae* ATCC 51700 and *P. gingivalis* (W50 and ATCC 33277) were labeled with either fluorescein isothiocyanate (FITC; Life Sciences) or pHrodo Red succinimidyl ester (pHrodo; Life Sciences). The mean fluorescence intensities (MFIs) were measured for FITC and pHrodo on all bacteria used and found to be comparable (data not shown). Bacteria were grown to late exponential phase and harvested by centrifugation (9,000 × *g*, 30 min, 4°C) and then washed twice with PBS. Bacteria were resuspended at 3×10^9 bacteria/ml in PBS containing 0.1 mg/ml FITC and then incubated for 1 h at 37°C, with no light, and with gentle mixing. Labeled bacteria were washed three times with PBS before being resuspended in incomplete, indicator-free Eagle minimal essential medium (Gibco) at a cell density of 6×10^9 bacteria/ml. For pHrodo labeling, the bacteria were resuspended at 3×10^9 bacterial/ml in 100 mM sodium bicarbonate (pH 8.5) after harvesting and washing. pHrodo was added to the bacteria at a concentration of 0.5 mM, followed by incubation for 1 h at room temperature, with no light, and with gentle mixing. Labeled bacteria were then washed three times with PBS and resuspended at 3×10^9 bacteria/ml in PBS before being snap-frozen in liquid nitrogen and stored at −80°C.

Binding of bacteria to oral mucosal epithelial cells. Oral keratinocyte OKF6 cells (oral mucosal epithelial cells [29]; kindly provided by James Rheinwald, Harvard Institute of Medicine) were cultured in K-sfm medium (Life Technologies) containing 25 μg/ml bovine pituitary factor, 0.2 ng/ml epidermal growth factor, 0.3 mM $CaCl_2$, and 100 IU/ml penicillin-streptomycin. OKF6 cells were seeded into a 24-well plate at 5×10^5 cells per well, followed by incubation overnight at 37°C in 5% (vol/vol) CO_2. FITC-labeled bacteria were resuspended in antibiotic- and serum-free culture medium and added to the cell monolayers in increasing bacterium/cell ratios (BCRs), followed by incubation for 90 min at 37°C in 5% (vol/vol) CO_2. Bacteria were also added to the cell monolayers after being treated with 5 mM *N*-α-tosyl-L-lysine chloromethyl ketone hydrochloride (TLCK; Sigma-Aldrich) in PBS for 30 min at 37°C. TLCK is an irreversible inhibitor of serine proteases. The supernatant was removed from the cell monolayers containing the unbound bacteria. The cell monolayer was detached from the plate using 0.25% trypsin-EDTA (Sigma) and washed (1× K-sfm culture medium), and the adherence of the FITC-labeled bacteria to the epithelial cells was determined by flow cytometry (FC500; Beckman Coulter) as previously described (30). The FC500 was equipped with an argon ion laser operating at an excitation wavelength of 488 nm and a red solid state diode laser operating at 635 nm. The fluorescence was measured through a 525-nm filter (FITC, FL1). A typical forward- and side-scatter gate was set to exclude dead cells and aggregates, and a total of 3×10^4 events in the gate were collected. Flow cytometry data were analyzed using Kaluza flow cytometry analysis software version 1.1 (Beckman Coulter). A Student *t* test was used to determine statistical differences, and a *P* value of <0.05 was considered significant.

Mouse periodontitis model. BALB/c mice were obtained from the Walter and Eliza Hall Institute animal facility and were housed in specific-pathogen-free conditions at the Biological Research Facility in the Royal Dental Hospital of Melbourne. The murine periodontitis model protocol was adapted from that previously described (21) and was approved by the

University of Melbourne Ethics Committee for Animal Experimentation. Female BALB/c mice (10 per experimental group, 6 to 8 weeks old) were orally inoculated four times in one experiment or eight times in a separate experiment, each inoculation 2 days apart, with 10^{10} viable *P. gingivalis* W50 cells or *P. gulae* ATCC 51700 cells (25 μl) per inoculation. The mice were killed 8 weeks after the first oral inoculation (50 and 42 days after the final inoculation, for four and eight inoculations, respectively), and the maxillae were removed and processed as previously described (21).

Bacterium-induced apoptosis and cell death of oral epithelial cells. Oral keratinocyte (OKF6) cells were removed from tissue culture flasks with 0.25% trypsin-EDTA solution (Sigma) and resuspended in antibiotic-free culture medium at 10^6 cells/ml and allowed to recover for 1 h at 37°C in 5% (vol/vol) CO_2. The removal of adherent cells can damage the cell membrane and cause false-positive results, and 1 h of incubation was found to reverse any transient trypsin-induced membrane disruption. Increasing ratios of *P. gulae* ATCC 51700 and *P. gingivalis* (W50 and ATCC 33277) were added to the cell suspensions, which were then incubated at 37°C in 5% (vol/vol) CO_2 for 1 h. The levels of OKF6 cell apoptosis and cell death were determined using a Yo-Pro-1 and PI flow cytometry kit (Life Sciences) as recommended by the manufacturer. Yo-Pro-1 is a green fluorescent dye that can enter the cell during the early stages of apoptosis, when the cytoplasmic membrane becomes slightly permeable. PI is a red fluorescent dye that can only enter cells that are dead; thus, apoptotic cells were observed as green fluorescent cells, dead cells were observed as green and red, and healthy cells showed little or no fluorescence. Fluorescence was measured on the FC500 (Beckman Coulter), using a 525-nm filter for green fluorescence (FL1) and a 575-nm filter for red fluorescence (FL2). A Student *t* test was used to determine statistical differences, and a *P* value of <0.05 was considered significant.

Phagocytosis assay. pHrodo is a novel pH-sensitive fluorochrome that has been used to examine phagocytosis (31). RAW 264.7 (ATCC TIB-71) cells, a murine macrophage cell line, were used to examine phagocytosis of *P. gulae* ATCC 51700 and *P. gingivalis* (W50 and ATCC 33277). RAW 264.7 cells were cultured in RPMI 1640 (Sigma) containing 25 mM L-glutamine, 10% (vol/vol) heat-inactivated fetal calf serum, and 100 IU/ml penicillin-streptomycin. Adherent macrophages were removed by using 0.25% trypsin-EDTA and resuspended in antibiotic- and serum-free RPMI at 1.5×10^6 cells/ml. pHrodo-labeled bacteria were added in increasing ratios of bacteria to cells, followed by incubation for 1 h or 24 h at 37°C in 5% (vol/vol) CO_2. After incubation, the cells were washed twice and resuspended in PBS for analysis by flow cytometry on the FC500 (Beckman Coulter). Typical forward- and side-scatter gates were set to exclude dead cells and aggregates. A total of 3×10^4 events in the gate were collected, and phagocytosis was identified as pHrodo-positive cells (pHrodo fluorescence was measured using a 575-nm filter; FL2). Cells and bacteria incubated on ice rather than at 37°C were used as negative controls. A Student *t* test was used to determine statistical differences, and a *P* value of <0.05 was considered significant.

Cytokine assay. *P. gulae* ATCC 5170 and *P. gingivalis* (W50 and ATCC 33277) were harvested from liquid culture during late exponential growth phase and added at increasing ratios (20:1, 80:1, and 160:1) to 10^6 macrophages (RAW 264.7)/ml before being incubated for 90 min at 37°C in 5% (vol/vol) CO_2 in antibiotic-free, serum-free RPMI containing 25 mM L-glutamine. After incubation, the cells were centrifuged at $300 \times g$ to pellet the macrophages but not the bacteria, and the cell pellet was resuspended and washed in culture media. Macrophages were then incubated for 24 h at 37°C in 5% CO_2, the supernatants were collected, and the particulates were removed by centrifuged at $9{,}000 \times g$ for 30 min. The cytokine levels in the supernatants were measured using a Bio-Plex Pro mouse cytokine standard 23-Plex, Group 1 kit (Bio-Rad, New South Wales, Australia) on a Bio-Plex 200 System (Bio-Rad) as previously described (32) and according to the manufacturer's instructions. A Student *t* test was used to determine statistical differences, and a *P* value of <0.05 was considered significant.

RESULTS

***P. gulae* has Arg-X and Lys-X protease activity that is critical for epithelial cell adhesion.** A major virulence factor of the human periodontal pathogen *P. gingivalis* is the presence of Arg-X and Lys-X proteolytic activity. As such, we initially measured the Arg-X and Lys-X protease activities of a number of *Porphyromonas* species commonly isolated from companion animals: *P. asaccharolytica*, *P. circumdentaria*, *P. endodontalis*, *P. levii*, *P. gulae*, *P. macacae*, *P. catoniae*, and *P. salivosa*. Of these, only *P. gulae* exhibited the specific protease activity. A BLASTN search was performed using RgpA, RgpB, and Kgp gingipain gene sequences from *P. gingivalis* (ATCC 33277) against the publicly available draft genome sequences of the seven species that did not exhibit Arg-X or Lys-X protease activity, and no significant similarities were found. We then compared the activity for *P. gulae* to that for the human pathogens *P. gingivalis* W50 and ATCC 33277 (Fig. 1A). *P. gulae* ATCC 51700 exhibited a level of Arg-X protease activity similar to that of *P. gingivalis* W50 and lower than that of ATCC 33277, but it had a significantly ($P < 0.0001$) higher Lys-X protease activity than either *P. gingivalis* strain.

A BLASTN search of the 12 draft *P. gulae* genomes available (33) confirmed that they did contain the *rgpA*, *rgpB*, and *kgp* gingipain genes. Since it has been suggested in the literature that the *P. gulae* genome contains the *rgpA* and *rgpB* genes but not the *kgp* gene (34), we explored the presence of this gene in more detail. We sequenced *P. gulae* ATCC 51700 and confirmed that it possessed a 5,193-bp gene encoding a gingipain catalytic domain and associated cleaved adhesin domains (CADs) that had a high level of identity to the *P. gingivalis* W83 *kgp* gene that encodes the Lys-specific gingipain and associated CADs (see Fig. S1 in the supplemental material). All three essential catalytic residues were conserved in the *P. gulae* ATCC 51700 sequence (see Fig. S1 in the supplemental material). We then examined the recently published draft genome sequences of 12 *P. gulae* strains (33) for the presence of a *kgp* gene encoding the catalytic domain of the Lys-specific gingipain. All 12 draft genomes contained a *kgp* gene that was nearly identical to that found in that *P. gulae* ATCC 51700 (see Fig. S2 in the supplemental material). All three essential catalytic residues were conserved in all *P. gulae* strains. Two isoforms of the Kgp catalytic domain were seen, with 13 specific amino acid substitutions found in strains JRAK01000000 and JRAE01000000 relative to the other strains.

We then examined the ability of *P. gulae* ATCC 51700 to autoaggregate since this, along with Arg-X and Lys-X protease activity and binding to oral epithelial cells, has been linked to the virulence of the human periodontal pathogen (28, 30). *P. gulae* ATCC 51700 was found, by use of the turbidity reduction assay, to have a higher rate of autoaggregation than both *P. gingivalis* species, reaching a significantly higher level of autoaggregation at 80 min (Fig. 1B).

To examine binding to oral epithelial cells (OKF6 cells), *P. gulae* ATCC 51700 and *P. gingivalis* (W50 and ATCC 3277) were labeled with a fluorophore, FITC, and the level of bound bacteria was determined using flow cytometry. Increasing ratios of bacteria to cells were used to examine both the percentage of oral epithelial cells with adhered bacteria and the MFI, an indication of how many bacteria are bound per oral epithelial cell. The binding of bacteria was observed as an increase in fluorescence (FITC) of oral epithelial cells, and as the bacterium/cell ratio (BCR) increased there was a corresponding increase in the percentages of epithelial

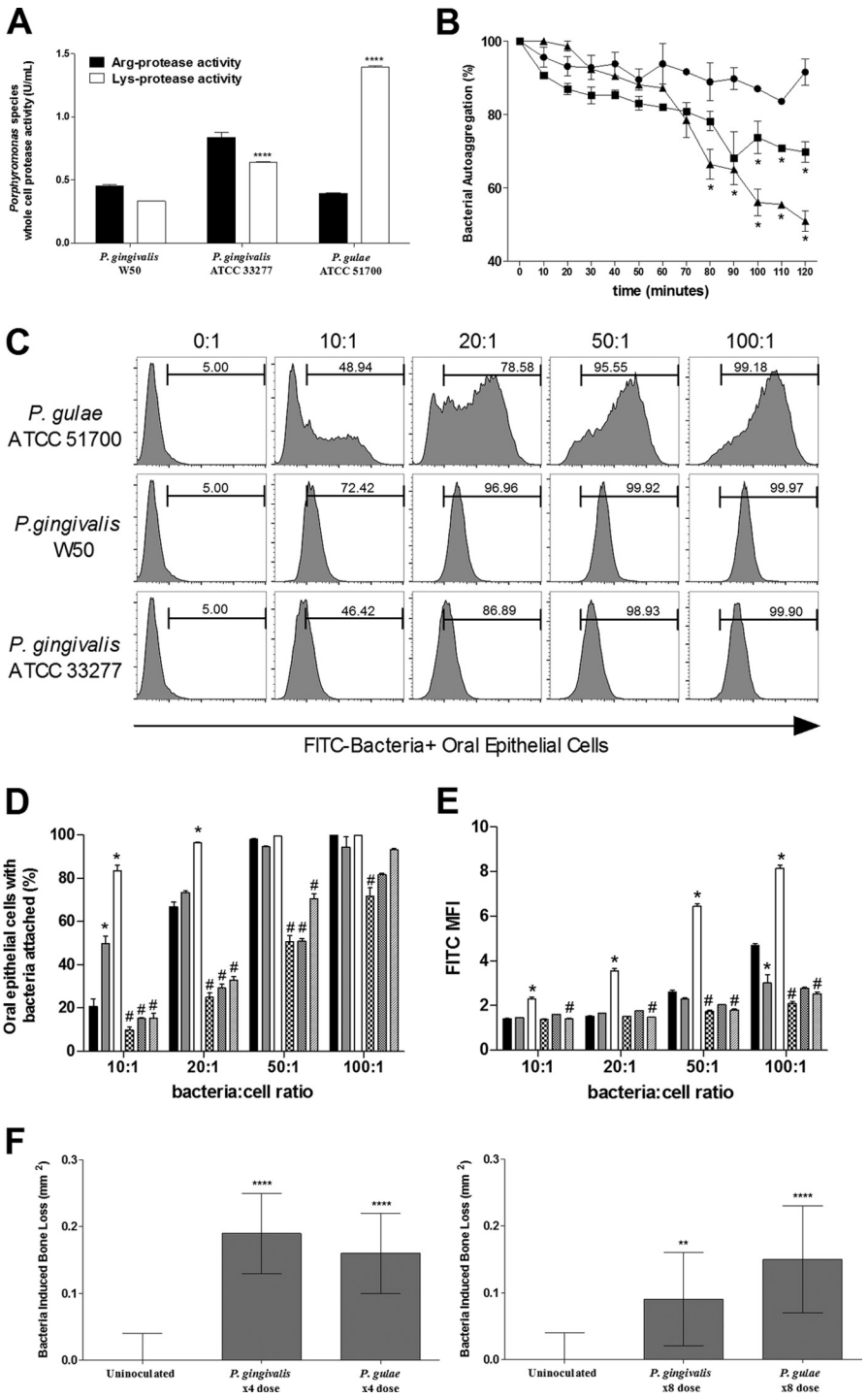

FIG 1 *P. gulae* binds to oral epithelial cells, autoaggregates, and has Arg- and Lys-specific proteolytic activity. (A) The proteolytic activity was determined using BA*p*NA (arginine, ■) and Lys*p*NA (lysine, □) substrates. *P. gulae* whole cells (10^8 bacteria/ml) showed significantly more lysine activity than *P. gingivalis* W50 (10^8 bacteria/ml) and *P. gingivalis* ATCC 33277 (10^8 bacteria/ml). All data are expressed as U/ml of proteolytic activity from two separate experiments ($n = 6$). Means ± the standard errors of the mean (SEM) are shown (****, $P < 0.0001$). (B) Autoaggregation was measured as the decrease in optical density, with an OD_{650} set at an initial 1.00 for each bacterium. *P. gingivalis* W50 (●) displayed minimal autoaggregation, whereas *P. gingivalis* ATCC 33277 (■) and *P. gulae* ATCC 51700 (▲) showed significantly more autoaggregation. Data are representative of three separate experiments. Means ± the SEM are shown (*, $P < 0.05$, *P. gulae* and *P. gingivalis* ATCC 33277 versus *P. gingivalis* W50 [$n = 3$] and *P. gulae* and *P. gingivalis* ATCC 33277 versus *P. gingivalis* W50 [$n = 3$]). (C to E) *P. gingivalis* (W50 and ATCC 33277) and *P. gulae* ATCC 51700 were labeled with FITC and examined for their ability to bind to oral epithelial cells in increasing ratios of bacteria to epithelial cells. All bacteria were found to bind to oral epithelial cells (C); however, *P. gulae* ATCC 51700 (□) bound at a greater rate than did *P. gingivalis* ATCC 33277 (▩) and *P. gingivalis* W50 (■), as measured by the percentage of FITC-positive cells (D) and the MFI (E). Bacteria treated with TLCK—*P. gulae* ATCC 51700 (▨), *P. gingivalis* W50 (▩), and *P. gingivalis* ATCC 33277 (▩)—showed a decrease in binding. Data are expressed as the percentages of FITC-positive cells or the MFIs and are representative of three separate experiments. Means ± the SEM are shown (*, $P < 0.05$ [*P. gulae* and *P. gingivalis* ATCC 33277 versus *P. gingivalis* W50]; #, $P < 0.05$ [TLCK-treated bacteria versus non-TLCK-treated bacteria]; $n = 3$). (F) BALB/c mice were orally inoculated with either four or eight doses of 10^{10} *P. gulae* ATCC 51700 or *P. gingivalis* W50 cells in two separate experiments. Maxillary bone loss was measured 8 weeks after the first inoculation; data are expressed as bacterium-induced bone loss in mm^2. Means ± the SEM are shown (**, $P < 0.005$; ****, $P < 0.00005$ [*P. gulae* and *P. gingivalis* W50 versus uninoculated; $n = 10$]).

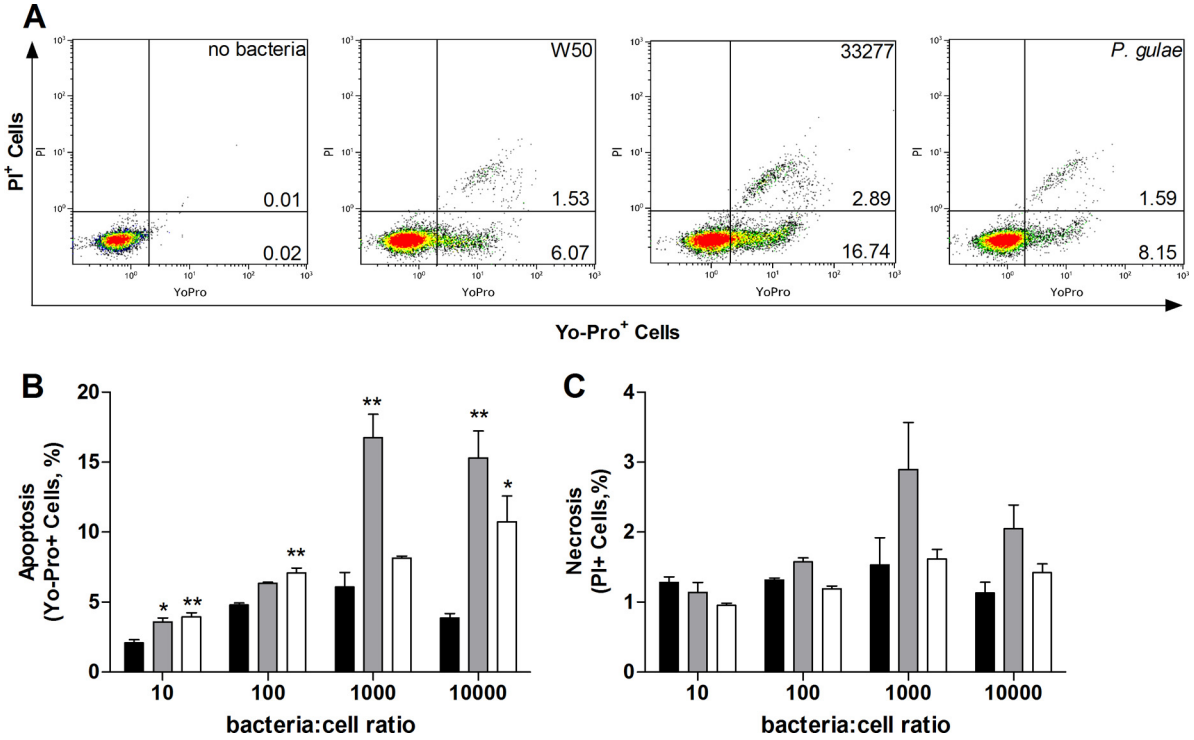

FIG 2 *P. gulae* induces apoptosis and death in oral epithelial cells. (A) Apoptosis was measured as an increase in green fluorescence (Yo-Pro-1), and cell death was measured as an increase in green and red (PI) fluorescence. (B) All bacteria tested induced apoptosis; however, *P. gingivalis* ATCC 33277 (▩) and *P. gulae* ATCC 51700 (□) induced significantly more apoptosis than did *P. gingivalis* W50 (■). (C) All bacteria induced similar levels of cell death (PI) at the time point measured. Means ± the SEM are shown (*, $P < 0.05$; **, $P < 0.005$ [*P. gulae* and *P. gingivalis* ATCC 33277 versus *P. gingivalis* W50; $n = 3$]).

cells with bacteria attached for *P. gulae* and *P. gingivalis* (Fig. 1C). At BCRs of 10:1 and 20:1, *P. gulae* ATCC 51700 and *P. gingivalis* ATCC 33277 were found to adhere to a lower percentage of oral epithelial cells than did *P. gingivalis* W50 (Fig. 1D). However, at BCRs of 50:1 and above, all (100%) oral epithelial cells had *P. gulae* or *P. gingivalis* attached (Fig. 1D). Interestingly, unlike the *P. gingivalis* strains, which adhered to oral epithelial cells as a single population, *P. gulae* ATCC 51700 exhibited high and low binding cell populations at BCRs of 10:1 and 20:1 (Fig. 1D). Despite the variation in population binding profiles at all of the ratios examined, significantly ($P < 0.01$) more *P. gulae* ATCC 51700 cells were found to be bound per oral epithelial cell than either *P. gingivalis* W50 or ATCC 33277 cells, as reflected by higher MFI values (Fig. 1E). Bacteria were also incubated with TLCK in this experiment to inactivate their protease activity, thus highlighting the role these proteases have in binding. Protease inactivation on *P. gulae* ATCC 51700 significantly reduced its ability to bind to oral epithelial cells (Fig. 1D and E). This was also observed for *P. gingivalis* W50 and ATCC 33277.

Finally, we show that *P. gulae* ATCC 51700 induced alveolar bone loss in the mouse periodontitis model and compared the level of bone loss to that induced by *P. gingivalis* W50. We inoculated BALB/c mice with 10^{10} *P. gulae* ATCC 51700 or *P. gingivalis* W50 cells, 2 days apart, with either four or eight doses, in two separate experiments. *P. gulae* was found to induce alveolar bone loss in both dosing regime experiments, and the level of bone loss was not significantly different from that induced by *P. gingivalis* W50 using the same dose regime (Fig. 1F).

***P. gulae* induces cell death of oral epithelial cells.** Periodontal pathogens have previously been shown to induce epithelial cell apoptosis (35). In this study, we examined and compared the ability of *P. gulae* ATCC 51700 to induce apoptosis of oral epithelial cells to that of *P. gingivalis* (W50 and ATCC 33277). After incubation for 60 min, all three bacterial strains induced apoptosis and cell death, as indicated by the increase in Yo-Pro-1 and PI fluorescence (Fig. 2A). *P. gulae* ATCC 51700 induced high levels of apoptosis of oral epithelial cells, which were significantly higher than that induced by *P. gingivalis* W50 but similar to that observed with *P. gingivalis* ATCC 33277 (Fig. 2B). A significant ($P < 0.05$) and positive correlation was found between the number of bacteria bound to the oral epithelial cells and the level of apoptosis observed for *P. gulae* ATCC 51700 ($R^2 = 0.9279$) and *P. gingivalis* ATCC 33277 ($R^2 = 0.7791$) (Fig. 2B). At the time point and BCRs examined, all of the bacteria induced similar levels of cell death, as determined from the PI fluorescence (Fig. 2C).

Phagocytosis of *P. gulae*. Macrophages are an important component of the innate immune system, and their cell numbers are higher in the gingival tissues of chronic periodontitis patients than in gingival tissues of healthy subjects (36, 37). These phagocytic cells play a role in bacterial clearance and immune surveillance and, as such, it is important to determine whether *P. gulae* was recognized and phagocytosed by macrophages. *P. gulae* ATCC 51700 and *P. gingivalis* (W50 and ATCC 33277) were labeled with pHrodo, a novel fluorogenic dye that only fluoresces in acidic conditions, such as those found within the phagosome, making it ideal for measuring phagocytosis. The mouse macrophage cell line RAW 264.7 was found to phagocytose *P. gulae* ATCC 51700 and both *P. gingivalis* W50 and ATCC 33277 (Fig. 3A). At a BCR of

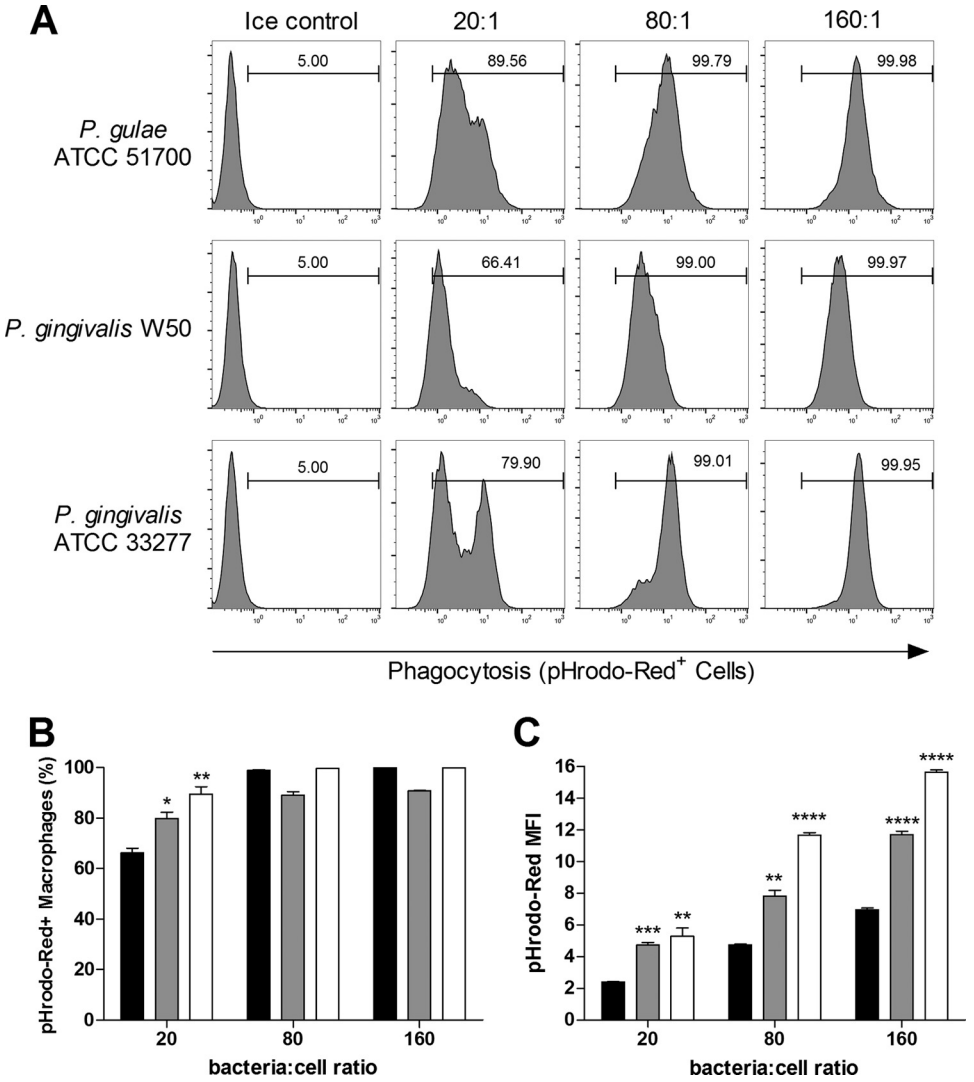

FIG 3 *P. gulae* is phagocytosed more readily than *P. gingivalis*. *P. gingivalis* (W50 and ATCC 33277) and *P. gulae* ATCC 51700 were labeled with pHrodo and examined for their ability to be phagocytosed by mouse macrophages (RAW 264.7) at increasing bacterium/cell ratios (BCRs). (A to C) Mouse macrophages can phagocytose both bacterial strains, as determined by an increase in pHrodo fluorescence (A); however, *P. gulae* ATCC 51700 (□) and *P. gingivalis* ATCC 33277 (■) were more readily phagocytosed than *P. gingivalis* W50 (■), as determined by the percentages of pHrodo-positive cells (B) and the MFIs (C). Data are expressed as the percentages of pHrodo-positive cells or the MFI. Means ± the SEM are shown (*, $P < 0.05$; **, $P < 0.005$; ***, $P < 0.0005$; ****, $P < 0.00005$ [*P. gulae* and *P. gingivalis* ATCC 33277 versus *P. gingivalis*; $n = 3$]).

20:1, the percentages of macrophages that were pHrodo positive for *P. gulae* were significantly higher than those that were pHrodo positive for *P. gingivalis* ATCC 33277 or W50 (Fig. 3B). Furthermore, as indicated by the MFI, significantly more *P. gulae* and *P. gingivalis* strain ATCC 33277 were phagocytosed per macrophage than *P. gingivalis* strain W50 (Fig. 3C). All bacteria tested showed a positive correlation (*P. gulae*, $R^2 = 0.9992$; *P. gingivalis* W50, $R^2 = 0.9999$; and *P. gingivalis* ATCC 33277, $R^2 = 0.9712$) between the number of bacteria and the MFI value of the macrophages (bacteria phagocytosed) (Fig. 3C).

***P. gulae* induces pro- and anti-inflammatory cytokines in macrophages.** The macrophage cytokine response to bacteria is one of the early defining events that shape the subsequent immune response. In this study, we examined the 24-h cytokine response from the murine macrophage cell line RAW 264.7 when incubated with *P. gulae* ATCC 51700. Bacteria were incubated at increasing cell ratios with macrophages for 90 min before being removed, since initial studies found that sustained (24-h) incubation of macrophages with *P. gulae* resulted in significantly high levels of cell death (data not shown), as seen with oral epithelial cells (Fig. 2), which were similar to that induced by *P. gingivalis*. At 24 h after incubation (90 min) with *P. gulae*, the RAW 264.7 cells were examined for apoptosis and necrosis, which was found to be <5%, indicating that the cytokines being produced were not due to large amounts of macrophage apoptosis or death. *P. gulae* induced the proinflammatory cytokines interleukin-1α (IL-1α), IL-1β, IL-3, IL-6, IL-12p40, IL-12p70, IL-17, tumor necrosis factor alpha (TNF-α), and gamma interferon (IFN-γ). The levels of these cytokines were significantly lower than those induced by *P. gingivalis* W50 but comparable to those with *P. gingivalis* ATCC 33277, with the exception of IL-1α, TNF-α, and IL-6 (Fig. 4). All bacteria tested induced comparable levels of IL-1α and TNF-α;

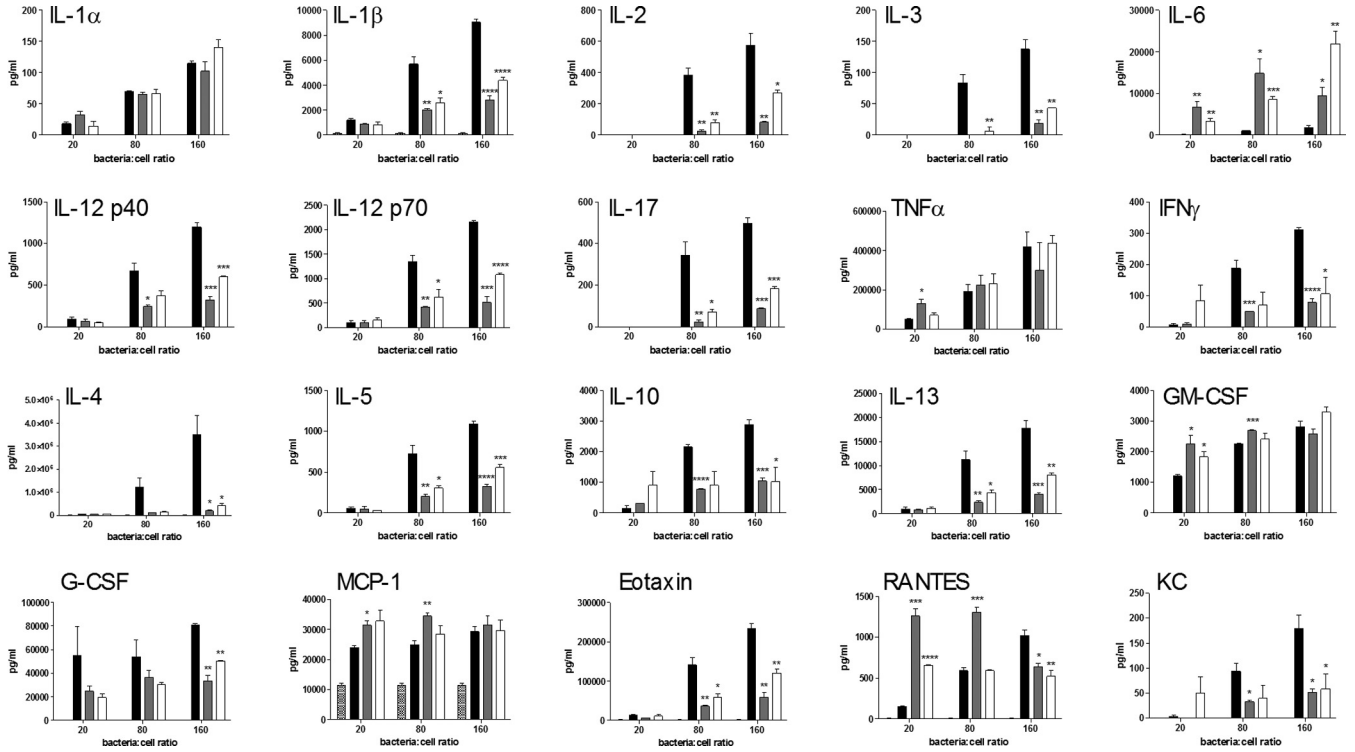

FIG 4 Macrophage cytokine response to *P. gulae*. RAW 264.7 macrophages were incubated with no bacteria (▨), *P. gulae* ATCC 51700 (□), *P. gingivalis* ATCC 33277 (■), or *P. gingivalis* W50 (■) for 90 min before the cells were centrifuged and the bacterium-containing supernatant was removed. The cytokine responses were measured after 24 h of incubation. Data are expressed as pg/ml. Means ± the SEM are shown (*, $P < 0.05$; **, $P < 0.005$; ***, $P < 0.0005$; ****, $P < 0.00005$ [*P. gulae* and *P. gingivalis* ATCC 33277 versus *P. gingivalis*; $n = 3$]).

however, *P. gulae* ATCC 51700 and *P. gingivalis* ATCC 33277 induced significantly higher levels of IL-6 than did *P. gingivalis* W50. Of note, at the 160:1 ratio *P. gulae* ATCC 51700 induced significantly more IL-6 than either *P. gingivalis* strains. Interestingly, *P. gulae* ATCC 51700 also induced significantly lower levels of the anti-inflammatory cytokines (IL-4, IL-5, IL-10, and IL-13) than did *P. gingivalis* W50, but these were again similar to the results observed with *P. gingivalis* ATCC 33277 (Fig. 4). At lower BCRs, *P. gulae* ATCC 51700 and *P. gingivalis* 33277 induced higher levels of the growth factor granulocyte-macrophage colony-stimulating factor and the chemokines MCP-1 and RANTES (Fig. 4); however, this increase was less dramatic at higher cell ratios. *P. gingivalis* W50 induced significantly higher levels of the growth factor granulocyte colony-stimulating factor and the chemokines eotaxin and KC than the other bacteria (Fig. 4). Overall, *P. gulae* ATCC 51700 induced a macrophage cytokine profile similar to that induced by *P. gingivalis* ATCC 33277. The levels of cytokines produced by *P. gulae* ATCC 51700 were typically greater than those produced by *P. gingivalis* ATCC 33277 but lower than those produced by *P. gingivalis* W50.

DISCUSSION

Periodontitis is a significant problem in companion animals, and several species of black-pigmented anaerobic bacteria have been isolated from the oral cavities of animals (3). In humans, the black-pigmented anaerobe *P. gingivalis* produces extracellular proteases (Arg-X and Lys-X specificity) that are major virulence factors and are strongly associated with disease progression and severity (38). Of the eight companion animal *Porphyromonas* species tested, only *P. gulae* ATCC 51700 exhibited Arg-X and Lys-X proteolytic activity, and it was found to have a significantly higher Lys-X activity than *P. gingivalis* W50 and ATCC 33277 (Fig. 1). Given the importance of these proteases in *P. gingivalis*-induced periodontitis, we hypothesized that the higher levels of Lys-X expression by *P. gulae* ATCC 51700 may lead to increased host immune dysregulation and tissue destruction. Indeed, previous research from our laboratory has shown that the Lys-specific activity of *P. gingivalis* associated with Kgp (Lys-specific gingipain) is one of the key determinants of virulence (39). We sequenced *P. gulae* ATCC 51700 and confirmed that it did contain the *rgpA*, *rgpB*, and *kgp* gingipain genes. The *kgp* gene sequence exhibited a high sequence similarity to that of *P. gingivalis* W83 (see Fig. S1 and S2 in the supplemental material). Our findings are not in agreement with those of O'Flynn et al. (34) who state that the *P. gulae* strains in their study contained *rgpA* and *rgpB* but not the *kgp* gene. Using the *kgp* gene sequence as a search item we have shown that the *P. gulae* strains reported by O'Flynn et al. (34) and the *P. gulae* sequences reported by Coil et al. (33) all contain the *kgp* gene (see Fig. S2 in the supplemental material). Thus, our data show that all *P. gulae* strains isolated and sequenced from companion animals with periodontitis contain the *rgpA*, *rgpB*, and *kgp* gingipain genes, which are major virulence factors of the human periodontal pathogen *P. gingivalis* (38). Alveolar bone loss is a hallmark of periodontitis, and the human pathogen *P. gingivalis* has been shown to induce alveolar bone loss in murine models of disease. We have confirmed that oral inoculation of *P. gulae* ATCC 51700 in mice induces alveolar bone loss comparable to that with *P.*

gingivalis, consistent with *P. gulae* being an oral pathogen capable of inducing periodontitis in companion animals.

The ability of periodontal pathogenic bacteria to adhere to and invade host cells is a major virulence factor, and fimbriae are important for their adhesion to oral epithelial cells and fibroblasts (40–43). In this study, we examined two strains of *P. gingivalis*: W50, a sparsely fimbriated strain with type IV fimbriae, and ATCC 33277, a highly fimbriated strain with type I fimbriae (38). *P. gulae* ATCC 51700 has been shown to express a 41-kDa fimbrial protein (FimA) that has molecular and antigenic properties similar to those of the 41-kDa fimbrial protein found on *P. gingivalis* ATCC 33277 (17). *P. gulae* has also been reported to have a secondary fimbrial protein of differing size (53 kDa) and antigenicity from the FimA protein (44). In our study, the binding capacity of *P. gulae* ATCC 51700 was examined using the oral epithelial cell line OKF6, with two measurements of adherence used: the percentage of cells with bacteria attached and the MFI, an indication of how many bacteria are bound per epithelial cell. At low BCRs, the fimbriated *P. gulae* ATCC 51700 and *P. gingivalis* ATCC 33277 adhered to a lower percentage of epithelial cells than the sparsely fimbriated *P. gingivalis* W50. However, *P. gulae* ATCC 51700 had significantly higher MFI values at all of the BCRs examined. Higher MFI values suggest that the fimbriated forms of bacteria autoaggregate and thus that higher numbers of bacteria are able to adhere to individual cells. We showed here that both *P. gulae* ATCC 51700 and *P. gingivalis* ATCC 33277 autoaggregated (Fig. 1B). Interestingly, despite sharing similar FimA proteins, *P. gulae* ATCC 51700 exhibited higher MFI values than did *P. gingivalis* ATCC 33277. These data are not consistent with a previous study that examined the binding of these bacteria to primary human gingival epithelial cells (17); however, that study used a method that involved lysing the epithelial cells and subsequent determination of CFU on agar, thus measuring binding and invasion. Our flow cytometry method is likely to be more sensitive and not only reveals the percentages of cells with bacteria adhered/invaded but also gives an indication of how many bacteria are adhered/invaded per cell and is not dependent on a further growth assay to show the presence of bacteria. The Arg-X and Lys-X proteolytic activity appears to play a role in the binding of *P. gulae* ATCC 51700 to oral epithelial cells, as demonstrated by reduced binding when protease activity was inhibited. This has previously been shown with the adherence of *P. gingivalis* W50 to KB cells (30).

Direct damage of the oral epithelial cells may also contribute to the pathology of periodontitis in companion animals. In this study, we have shown that *P. gulae* ATCC 51700 induced significantly more apoptosis in oral epithelial cells (Fig. 2) than *P. gingivalis* W50. This increase may be due to *P. gulae* ATCC 51700 being fimbriated and thus able to bind to cells in greater numbers, similar to the fimbriated *P. gingivalis* ATCC 33277. In addition, the high level of Lys-specific proteolytic activity found on *P. gulae* ATCC 51700 may also contribute to apoptosis, which is consistent with previous reports on *P. gingivalis* (39).

The ability of *P. gulae* to induce inflammation and bone loss can be attributed to the subsequent host immune response to the bacterium. Epithelial cells would be the first host cell to encounter a *Porphyromonas* species in subgingival plaque but, as major immune cells, the bacterium would also have early contact with macrophages, which are critical effectors and regulators of both inflammation and the innate immune response. Macrophages are located throughout the tissues of the body and perform a surveillance function, phagocytosing bacteria in order to remove the pathogen and also to initiate the subsequent immune response (45). In humans, macrophages have been identified as a major cell type in the inflammatory infiltrate of the gingival tissue during chronic periodontitis (46). Chronic inflammation and tissue damage result when newly recruited "inflammatory" cells chronically enter the tissue, often initiated by the resident macrophages and other professional antigen-presenting cells (47). It is therefore important to ascertain what immune response *P. gulae* elicits from macrophages and whether these phagocytic cells can recognize, respond to, and phagocytose the bacteria. We examined whether the murine macrophage cell line RAW 264.7 was able to phagocytose pHrodo-labeled bacteria. When a macrophage ingests a pHrodo-labeled bacterium, the pathogen becomes trapped in a phagosome. As the phagosome matures and ultimately fuses with a lysosome, its interior becomes increasingly acidic (48), and it is this decrease in pH that increases the fluorescence intensity of the pHrodo dye (31). This dye allows us to definitively identify cells that have phagocytosed bacteria, rather than bacteria adhered to the surface or bacteria invading the host cell, since the pH of the cytoplasm is >7.0. *P. gulae* ATCC 51700 and *P. gingivalis* (W50 and ATCC 33277) were all recognized and phagocytosed by RAW 264.7 macrophages. However, at a lower BCR there was a significantly higher percentage of macrophages that were pHrodo positive for *P. gulae* ATCC 51700 or *P. gingivalis* ATCC 33277 than for *P. gingivalis* W50 (Fig. 3A and B). In this assay, the MFI can reflect two parameters: the number of bacteria ingested by the macrophage and the age of the phagosome. Macrophages incubated with the fimbriated *P. gulae* ATCC 51700 or *P. gingivalis* ATCC 33277 had a significantly higher MFI than macrophages incubated with the sparsely fimbriated *P. gingivalis* (W50). This suggests either that *P. gulae* ATCC 51700 and *P. gingivalis* ATCC 33277 are phagocytosed in greater numbers or that they are phagocytosed more rapidly. Given that we examined pHrodo fluorescence at 1 h, it is conceivable that *P. gulae* ATCC 51700 enters a phagosome earlier than *P. gingivalis* W50; thus, at 1 h *P. gulae* ATCC 51700 is present in a more mature, acidic phagosome. Although the kinetics of phagosome maturation differ greatly depending on the matter that is ingested and the type of cell being examined, these phagosomes can start to mature and become acidic within 10 to 30 min of formation (49, 50). Alternatively, given that highly fimbriated bacteria autoaggregate, aggregates of *P. gulae* ATCC 51700 and *P. gingivalis* ATCC 33277 may be phagocytosed, thus increasing the MFI.

One of the ways that macrophages modulate the resulting immune response to infection is to release chemokines, which in turn can signal for additional immune cells to traffic to the site of infection, and cytokines, which can drive a proinflammatory or anti-inflammatory response (45). As expected, *P. gulae* ATCC 51700 and *P. gingivalis* (W50 and ATCC 33277) induced a proinflammatory cytokine response from RAW 264.7 macrophages (Fig. 4). Interestingly *P. gulae* ATCC 51700 induced significantly lower expression of IL-1α, IL-1β, IL-2, IL-3, IL-12p40, IL-12p70, IL-17, and IFN-γ than did *P. gingivalis* W50, indicating that it may not induce an inflammatory response that is as robust as that induced by *P. gingivalis* W50. However, all bacteria tested induced similar levels of TNF-α. A number of recent studies suggest that TNF-α has a significant role in bone loss during periodontitis. The administration of recombinant human TNF-α to rats has been shown to acceler-

ate the progression of periodontitis (51), and TNF-α receptor knockout mice develop significantly less inflammation and alveolar bone loss (52). In contrast to these results, *P. gulae* ATCC 51700 induced significantly higher levels of IL-6 than did *P. gingivalis* (W50 and ATCC 33277). IL-6 is able to stimulate various biological processes, including antibody production, B cell differentiation, T cell activation, and osteoclast differentiation (53). IL-6 knockout mice have been shown to have decreased bone loss compared to wild-type mice in a *P. gingivalis* periodontitis model (54), suggesting that the expression of IL-6 is involved in alveolar bone resorption. The high levels of IL-6 induced by *P. gulae* ATCC 51700 observed in our study may be responsible for the significantly lower levels of other proinflammatory cytokines; IL-6 has been shown to downregulate the expression of other proinflammatory cytokines (55). Although *P. gingivalis* W50 appears to induce a greater proinflammatory cytokine response, it also induces a greater anti-inflammatory response. Indeed, the lower levels of protective, anti-inflammatory cytokines induced by *P. gulae* ATCC 51700 may lead to a greater inflammatory response and greater bone loss, particularly in the presence of IL-6 and TNF-α. Taken together, these data show that *P. gulae* ATCC 51700 induces a proinflammatory profile from macrophages with levels of the proinflammatory cytokines IL-1α, TNF-α, and IL-6 similar to or higher than those induced by *P. gingivalis* W50. Chemokines constitute a family of chemoattractant cytokines that play a major role in selectively recruiting monocytes, neutrophils, and lymphocytes. In the present study, we showed that several chemokines are released by macrophages in response to *Porphyromonas* species. *P. gulae* ATCC 51700 induced high levels of monocyte chemoattractant protein-1 (MCP-1/CCL2), a key chemokine that regulates the migration and infiltration of monocytes/macrophages (56). Macrophages themselves can produce MCP-1 in order to attract more macrophages to a site of infection or inflammation and, indeed, elevated levels of MCP-1 have been reported in cases of chronic periodontal disease (57). *P. gulae* ATCC 51700 also induced the expression of KC (CXCL1) at levels similar to those induced by *P. gingivalis* ATCC 33277; however, the levels were significantly lower than those induced by *P. gingivalis* W50. KC is a potent chemoattractant for neutrophils (58), which is consistent with the well-established role of neutrophils in periodontal disease.

P. gulae has been implicated as a major pathogen in companion animal periodontitis by its association with disease. In this study, we examined several aspects of *P. gulae* virulence and its interaction with the host immune system. Of all the companion animal *Porphyromonas* species examined, *P. gulae* was the only species to express Arg- and Lys-specific proteolytic activity. Indeed, it had significantly more whole-cell lysine specific activity than the human periodontal pathogen *P. gingivalis*. *P. gulae* is fimbriated, sharing the FimA protein with *P. gingivalis* ATCC 33277, and as such is autoaggregated. *P. gulae* ATCC 51700 can adhere to oral epithelial cells in greater numbers than *P. gingivalis* W50 and this, coupled with greater Lys-specific proteolytic activity, may explain its increased ability to induce apoptosis and kill oral epithelial cells. *P. gulae* ATCC 51700 induced a predominantly proinflammatory cytokine profile from macrophages highlighted by similar levels of IL-1α and TNF-α and increased levels of IL-6 with decreased levels of anti-inflammatory cytokines. *P. gulae* has virulence characteristics that are associated with the human periodontal pathogen *P. gingivalis* and, as such, may play a key role in the pathology of periodontitis in animals.

ACKNOWLEDGMENTS

This study was supported by the Australian Government, Department of Industry, Innovation, and Science.

We thank Katrina Laughton for technical assistance.

FUNDING INFORMATION

This work, including the efforts of Eric C. Reynolds, was funded by Cooperative Research Centres, Australian Government Department of Industry (CRCs) (20080108).

REFERENCES

1. **Harvey CE.** 1998. Periodontal disease in dogs: etiopathogenesis, prevalence, and significance. Vet Clin North Am Small Anim Pract **28:**1111–1128. http://dx.doi.org/10.1016/S0195-5616(98)50105-2.
2. **Larsen J.** 2010. Oral products and dental disease. Compend Contin Educ Vet **32:**E1–E3.
3. **Allaker RP, de Rosayro R, Young KA, Hardie JM.** 1997. Prevalence of *Porphyromonas* and *Prevotella* species in the dental plaque of dogs. Vet Rec **140:**147–148. http://dx.doi.org/10.1136/vr.140.6.147.
4. **Boyce EN, Ching RJ, Logan EI, Hunt JH, Maseman DC, Gaeddert KL, King CT, Reid EE, Hefferren JJ.** 1995. Occurrence of gram-negative black-pigmented anaerobes in subgingival plaque during the development of canine periodontal disease. Clin Infect Dis **20**(Suppl 2)**:**S317–S319. http://dx.doi.org/10.1093/clinids/20.Supplement_2.S317.
5. **Forsblom B, Love DN, Sarkiala-Kessel E, Jousimies-Somer H.** 1997. Characterization of anaerobic, gram-negative, nonpigmented, saccharolytic rods from subgingival sites in dogs. Clin Infect Dis **25**(Suppl 2)**:**S100–S106. http://dx.doi.org/10.1086/516209.
6. **Kato Y, Shirai M, Murakami M, Mizusawa T, Hagimoto A, Wada K, Nomura R, Nakano K, Ooshima T, Asai F.** 2011. Molecular detection of human periodontal pathogens in oral swab specimens from dogs in Japan. J Vet Dent **28:**84–89. http://dx.doi.org/10.1177/089875641102800204.
7. **Oliver RC, Brown LJ.** 1993. Periodontal diseases and tooth loss. Periodontol 2000 **2:**117–127. http://dx.doi.org/10.1111/j.1600-0757.1993.tb00224.x.
8. **Barnard P.** 1993. National Oral Health Survey Australia 1987-88. Australian Government Printing Services, Canberra, Australia.
9. **Oliver RC, Brown LJ, Loe H.** 1998. Periodontal diseases in the United States population. J Periodontol **69:**269–278. http://dx.doi.org/10.1902/jop.1998.69.2.269.
10. **Byrne SJ, Dashper SG, Darby IB, Adams GG, Hoffmann B, Reynolds EC.** 2009. Progression of chronic periodontitis can be predicted by the levels of *Porphyromonas gingivalis* and *Treponema denticola* in subgingival plaque. Oral Microbiol Immunol **24:**469–477. http://dx.doi.org/10.1111/j.1399-302X.2009.00544.x.
11. **Lamont RJ, Jenkinson HF.** 1998. Life below the gum line: pathogenic mechanisms of *Porphyromonas gingivalis*. Microbiol Mol Biol Rev **62:**1244–1263.
12. **Hajishengallis G, Darveau RP, Curtis MA.** 2012. The keystone-pathogen hypothesis. Nat Rev Microbiol **10:**717–725. http://dx.doi.org/10.1038/nrmicro2873.
13. **Fournier D, Mouton C, Lapierre P, Kato T, Okuda K, Menard C.** 2001. *Porphyromonas gulae* sp. nov., an anaerobic, gram-negative coccobacillus from the gingival sulcus of various animal hosts. Int J Syst Evol Microbiol **51:**1179–1189. http://dx.doi.org/10.1099/00207713-51-3-1179.
14. **Senhorinho GN, Nakano V, Liu C, Song Y, Finegold SM, Avila-Campos MJ.** 2011. Detection of *Porphyromonas gulae* from subgingival biofilms of dogs with and without periodontitis. Anaerobe **17:**257–258. http://dx.doi.org/10.1016/j.anaerobe.2011.06.002.
15. **Senhorinho GN, Nakano V, Liu C, Song Y, Finegold SM, Avila-Campos MJ.** 2012. Occurrence and antimicrobial susceptibility of *Porphyromonas* spp. and *Fusobacterium* spp. in dogs with and without periodontitis. Anaerobe **18:**381–385. http://dx.doi.org/10.1016/j.anaerobe.2012.04.008.
16. **Yamasaki Y, Nomura R, Nakano K, Naka S, Matsumoto-Nakano M, Asai F, Ooshima T.** 2012. Distribution of periodontopathic bacterial

species in dogs and their owners. Arch Oral Biol **57:**1183–1188. http://dx.doi.org/10.1016/j.archoralbio.2012.02.015.
17. **Hamada N, Takahashi Y, Watanabe K, Kumada H, Oishi Y, Umemoto T.** 2008. Molecular and antigenic similarities of the fimbrial major components between *Porphyromonas gulae* and *P. gingivalis*. Vet Microbiol **128:**108–117. http://dx.doi.org/10.1016/j.vetmic.2007.09.014.
18. **Nomura R, Shirai M, Kato Y, Murakami M, Nakano K, Hirai N, Mizusawa T, Naka S, Yamasaki Y, Matsumoto-Nakano M, Ooshima T, Asai F.** 2012. Diversity of fimbrillin among *Porphyromonas gulae* clinical isolates from Japanese dogs. J Vet Med Sci **74:**885–891. http://dx.doi.org/10.1292/jvms.11-0564.
19. **Hardham J, Reed M, Wong J, King K, Laurinat B, Sfintescu C, Evans RT.** 2005. Evaluation of a monovalent companion animal periodontal disease vaccine in an experimental mouse periodontitis model. Vaccine **23:**3148–3156. http://dx.doi.org/10.1016/j.vaccine.2004.12.026.
20. **Hardham J, Dreier K, Wong J, Sfintescu C, Evans RT.** 2005. Pigmented-anaerobic bacteria associated with canine periodontitis. Vet Microbiol **106:**119–128. http://dx.doi.org/10.1016/j.vetmic.2004.12.018.
21. **O'Brien-Simpson NM, Pathirana RD, Paolini RA, Chen YY, Veith PD, Tam V, Ally N, Pike RN, Reynolds EC.** 2005. An immune response directed to proteinase and adhesin functional epitopes protects against *Porphyromonas gingivalis*-induced periodontal bone loss. J Immunol **175:**3980–3989. http://dx.doi.org/10.4049/jimmunol.175.6.3980.
22. **Hardham J, Sfintescu C, Evans RT.** 2008. Evaluation of cross-protection by immunization with an experimental trivalent companion animal periodontitis vaccine in the mouse periodontitis model. J Vet Dent **25:**23–27. http://dx.doi.org/10.1177/089875640802500107.
23. **Zoetis.** 2011. *Porphyromonas* pet owner communications. Zoetis Inc., Florham Park, NJ. https://www.zoetisus.com/_locale-assets/mcm-portal-assets/products/pdf/farrowsuregold/pfizerfrank/porphyromonas_petownercommunications.pdf.
24. **Pathirana RD, O'Brien-Simpson NM, Reynolds EC.** 2010. Host immune responses to *Porphyromonas gingivalis* antigens. Periodontol 2000 **52:**218–237. http://dx.doi.org/10.1111/j.1600-0757.2009.00330.x.
25. **O'Brien-Simpson NM, Paolini RA, Hoffmann B, Slakeski N, Dashper SG, Reynolds EC.** 2001. Role of RgpA, RgpB, and Kgp proteinases in virulence of *Porphyromonas gingivalis* W50 in a murine lesion model. Infect Immun **69:**7527–7534. http://dx.doi.org/10.1128/IAI.69.12.7527-7534.2001.
26. **Pathirana RD, O'Brien-Simpson NM, Veith PD, Riley PF, Reynolds EC.** 2006. Characterization of proteinase-adhesin complexes of *Porphyromonas gingivalis*. Microbiology **152:**2381–2394. http://dx.doi.org/10.1099/mic.0.28787-0.
27. **Untergasser A, Nijveen H, Rao X, Bisseling T, Geurts R, Leunissen JA.** 2007. Primer3Plus, an enhanced web interface to Primer3. Nucleic Acids Res **35:**W71–W74. http://dx.doi.org/10.1093/nar/gkm306.
28. **Nishiyama S, Murakami Y, Nagata H, Shizukuishi S, Kawagishi I, Yoshimura F.** 2007. Involvement of minor components associated with the FimA fimbriae of *Porphyromonas gingivalis* in adhesive functions. Microbiology **153:**1916–1925. http://dx.doi.org/10.1099/mic.0.2006/005561-0.
29. **Dickson MA, Hahn WC, Ino Y, Ronfard V, Wu JY, Weinberg RA, Louis DN, Li FP, Rheinwald JG.** 2000. Human keratinocytes that express hTERT and also bypass a p16(INK4a)-enforced mechanism that limits life span become immortal yet retain normal growth and differentiation characteristics. Mol Cell Biol **20:**1436–1447. http://dx.doi.org/10.1128/MCB.20.4.1436-1447.2000.
30. **Pathirana RD, O'Brien-Simpson NM, Visvanathan K, Hamilton JA, Reynolds EC.** 2007. Flow cytometric analysis of adherence of *Porphyromonas gingivalis* to oral epithelial cells. Infect Immun **75:**2484–2492. http://dx.doi.org/10.1128/IAI.02004-06.
31. **Miksa M, Komura H, Wu R, Shah KG, Wang P.** 2009. A novel method to determine the engulfment of apoptotic cells by macrophages using pHrodo succinimidyl ester. J Immunol Methods **342:**71–77. http://dx.doi.org/10.1016/j.jim.2008.11.019.
32. **Wong DM, Tam V, Lam R, Walsh KA, Tatarczuch L, Pagel CN, Reynolds EC, O'Brien-Simpson NM, Mackie EJ, Pike RN.** 2010. Protease-activated receptor 2 has pivotal roles in cellular mechanisms involved in experimental periodontitis. Infect Immun **78:**629–638. http://dx.doi.org/10.1128/IAI.01019-09.
33. **Coil DA, Alexiev A, Wallis C, O'Flynn C, Deusch O, Davis I, Horsfall A, Kirkwood N, Jospin G, Eisen JA, Harris S, Darling AE.** 2015. Draft genome sequences of 26 *Porphyromonas* strains isolated from the canine oral microbiome. Genome Announc **3:**e00187-15. http://dx.doi.org/10.1128/genomeA.00187-15.
34. **O'Flynn C, Deusch O, Darling AE, Eisen JA, Wallis C, Davis IJ, Harris SJ.** 2015. Comparative genomics of the genus *Porphyromonas* identifies adaptations for heme synthesis within the prevalent canine oral species *Porphyromonas cangingivalis*. Genome Biol Evol **7:**3397–3413. http://dx.doi.org/10.1093/gbe/evv220.
35. **O'Brien-Simpson NM, Pathirana RD, Walker GD, Reynolds EC.** 2009. *Porphyromonas gingivalis* RgpA-Kgp proteinase-adhesin complexes penetrate gingival tissue and induce proinflammatory cytokines or apoptosis in a concentration-dependent manner. Infect Immun **77:**1246–1261. http://dx.doi.org/10.1128/IAI.01038-08.
36. **Gemmell E, McHugh GB, Grieco DA, Seymour GJ.** 2001. Costimulatory molecules in human periodontal disease tissues. J Periodont Res **36:**92–100. http://dx.doi.org/10.1034/j.1600-0765.2001.360205.x.
37. **Lappin DF, Kjeldsen M, Sander L, Kinane DF.** 2000. Inducible nitric oxide synthase expression in periodontitis. J Periodont Res **35:**369–373. http://dx.doi.org/10.1034/j.1600-0765.2000.035006369.x.
38. **O'Brien-Simpson NM, Veith PD, Dashper SG, Reynolds EC.** 2004. Antigens of bacteria associated with periodontitis. Periodontol 2000 **35:**101–134. http://dx.doi.org/10.1111/j.0906-6713.2004.003559.x.
39. **Pathirana RD, O'Brien-Simpson NM, Brammar GC, Slakeski N, Reynolds EC.** 2007. Kgp and RgpB, but not RgpA, are important for *Porphyromonas gingivalis* virulence in the murine periodontitis model. Infect Immun **75:**1436–1442. http://dx.doi.org/10.1128/IAI.01627-06.
40. **Duncan MJ, Nakao S, Skobe Z, Xie H.** 1993. Interactions of *Porphyromonas gingivalis* with epithelial cells. Infect Immun **61:**2260–2265.
41. **Isogai H, Isogai E, Yoshimura F, Suzuki T, Kagota W, Takano K.** 1988. Specific inhibition of adherence of an oral strain of *Bacteroides gingivalis* 381 to epithelial cells by monoclonal antibodies against the bacterial fimbriae. Arch Oral Biol **33:**479–485. http://dx.doi.org/10.1016/0003-9969(88)90028-3.
42. **Njoroge T, Genco RJ, Sojar HT, Hamada N, Genco CA.** 1997. A role for fimbriae in *Porphyromonas gingivalis* invasion of oral epithelial cells. Infect Immun **65:**1980–1984.
43. **Pathirana RD, O'Brien-Simpson NM, Visvanathan K, Hamilton JA, Reynolds EC.** 2008. The role of the RgpA-Kgp proteinase-adhesin complexes in the adherence of *Porphyromonas gingivalis* to fibroblasts. Microbiology **154:**2904–2911. http://dx.doi.org/10.1099/mic.0.2008/019943-0.
44. **Oishi Y, Watanabe K, Kumada H, Ishikawa E, Hamada N.** 2012. Purification and characterization of a novel secondary fimbrial protein from *Porphyromonas gulae*. J Oral Microbiol http://dx.doi.org/10.3402/jom.v4i0.19076.
45. **Murray PJ, Wynn TA.** 2011. Protective and pathogenic functions of macrophage subsets. Nat Rev Immunol **11:**723–737. http://dx.doi.org/10.1038/nri3073.
46. **Moskow BS, Polson AM.** 1991. Histologic studies on the extension of the inflammatory infiltrate in human periodontitis. J Clin Periodontol **18:**534–542. http://dx.doi.org/10.1111/j.1600-051X.1991.tb00086.x.
47. **Nathan C, Ding A.** 2010. Nonresolving inflammation. Cell **140:**871–882. http://dx.doi.org/10.1016/j.cell.2010.02.029.
48. **Kinchen JM, Ravichandran KS.** 2008. Phagosome maturation: going through the acid test. Nat Rev Mol Cell Biol **9:**781–795. http://dx.doi.org/10.1038/nrm2515.
49. **de Chastellier C, Thilo L.** 1997. Phagosome maturation and fusion with lysosomes in relation to surface property and size of the phagocytic particle. Eur J Cell Biol **74:**49–62.
50. **Vieira OV, Botelho RJ, Rameh L, Brachmann SM, Matsuo T, Davidson HW, Schreiber A, Backer JM, Cantley LC, Grinstein S.** 2001. Distinct roles of class I and class III phosphatidylinositol 3-kinases in phagosome formation and maturation. J Cell Biol **155:**19–25. http://dx.doi.org/10.1083/jcb.200107069.
51. **Gaspersic R, Stiblar-Martincic D, Osredkar J, Skaleric U.** 2003. Influence of subcutaneous administration of recombinant TNF-alpha on ligature-induced periodontitis in rats. J Periodont Res **38:**198–203. http://dx.doi.org/10.1034/j.1600-0765.2003.01395.x.
52. **Garlet GP, Cardoso CR, Campanelli AP, Ferreira BR, Avila-Campos MJ, Cunha FQ, Silva JS.** 2007. The dual role of p55 tumour necrosis factor-alpha receptor in *Actinobacillus actinomycetemcomitans*-induced experimental periodontitis: host protection and tissue destruction. Clin Exp Immunol **147:**128–138. http://dx.doi.org/10.1111/j.1365-2249.2006.03260.x.
53. **Nibali L, Fedele S, D'Aiuto F, Donos N.** 2012. Interleukin-6 in oral

diseases: a review. Oral Dis **18:**236–243. http://dx.doi.org/10.1111/j.1601-0825.2011.01867.x.

54. **Baker PJ, Dixon M, Evans RT, Dufour L, Johnson E, Roopenian DC.** 1999. $CD4^+$ T cells and the proinflammatory cytokines gamma interferon and interleukin-6 contribute to alveolar bone loss in mice. Infect Immun **67:**2804–2809.
55. **Xing Z, Gauldie J, Cox G, Baumann H, Jordana M, Lei XF, Achong MK.** 1998. IL-6 is an antiinflammatory cytokine required for controlling local or systemic acute inflammatory responses. J Clin Invest **101:**311–320. http://dx.doi.org/10.1172/JCI1368.
56. **Deshmane SL, Kremlev S, Amini S, Sawaya BE.** 2009. Monocyte chemoattractant protein-1 (MCP-1): an overview. J Interferon Cytokine Res **29:**313–326. http://dx.doi.org/10.1089/jir.2008.0027.
57. **Gupta M, Chaturvedi R, Jain A.** 2013. Role of monocyte chemoattractant protein-1 (MCP-1) as an immune-diagnostic biomarker in the pathogenesis of chronic periodontal disease. Cytokine **61:**892–897. http://dx.doi.org/10.1016/j.cyto.2012.12.012.
58. **Kobayashi Y.** 2006. Neutrophil infiltration and chemokines. Crit Rev Immunol **26:**307–316. http://dx.doi.org/10.1615/CritRevImmunol.v26.i4.20.